WSRC-TR-93-322

664129

CORROSION OF STEEL IN SIMULATED NUCLEAR WASTES CONTAINING DIFFERENT NITRATE AND NITRITE CONCENTRATIONS (U)

by

J. Mickalonis

Westinghouse Savannah River Company
Savannah River Site
Aiken, South Carolina 29808

DOE Contract No. **DE-AC09-89SR18035**

WSRC-TR-93-322

CORROSION OF STEEL IN SIMULATED WASTE CONTAINING DIFFERENT NITRATE AND NITRITE CONCENTRATIONS (U)

By

J. I. Mickalonis

JULY, 1993

Westinghouse Savannah River Company
P. O. Box 616
Aiken, SC 29802

PREPARED FOR THE U.S. DEPARTMENT OF ENERGY UNDER CONTRACT DE-AC09-88SR18035
PRESENTLY UNDER CONTRACT DE-AC09-88SR18035

EMT
EQUIPMENT AND MATERIALS TECHNOLOGY

Keywords: Corrosion Monitoring
Waste Tanks
Polarization Test
Metallurgical Analysis

Retention: Permanent

CORROSION OF STEEL IN SIMULATED WASTE CONTAINING DIFFERENT NITRATE AND NITRITE CONCENTRATIONS (U)

by

J. I. Mickalonis

ISSUED: July, 1993

Authorized Derivative Classifier

D. Thomas Rankin

July 12, 1993
Date

SRTC SAVANNAH RIVER TECHNOLOGY CENTER, AIKEN, SC 29808
Westinghouse Savannah River Company
Prepared for the U. S. Department of Energy under Contract DE-AC09-88SR18035

DOCUMENT: WSRC-TR-93-322

TITLE: CORROSION OF STEEL IN SIMULATED WASTE CONTAINING DIFFERENT NITRATE AND NITRITE CONCENTRATIONS (U)

APPROVALS

Bruce J Wiersma DATE: 7-9-93

B. J. Wiersma, TECHNICAL REVIEWER
MATERIALS TECHNOLOGY SECTION

Nathaj Iyer DATE: 7-9-93

N. C. Iyer, ACTING MANAGER
MATERIALS APPL. & CORR. TECH. GROUP
MATERIALS TECHNOLOGY SECTION

D. Thomas Rankin for DATE: 7-12-93

T. L. Capeletti, MANAGER
MATERIALS TECHNOLOGY SECTION

TABLE OF CONTENTS

	PAGE #
EXECUTIVE SUMMARY	i
INTRODUCTION	1
EXPERIMENTAL PROCEDURES	1
RESULTS	3
Cyclic Polarization Test	3
Linear Polarization	5
Microstructural Analysis	6
Microstructural Characterization of Samples	6
Corrosion Morphology of Cyclic Polarization Disks	7
Corrosion Morphology of Linear Polarization Samples	8
CONCLUSIONS	9
REFERENCES	10
TABLES	11
FIGURES	15

J. I. Mickalonis
WSRC-TR-93-322
July, 1993

EXECUTIVE SUMMARY

Corrosion monitoring of the In-Tank Precipitation (ITP) and Extended Sludge Processing (ESP) waste tanks would provide a means to identify the corrosive state induced by processing conditions. An investigation was initiated to develop baseline data on the effect of changes in waste chemistry on corrosion processes of a waste tank which supports the evaluation of a new corrosion monitoring technique called electrochemical noise measurements (ENM).

Laboratory tests were conducted to verify the corrosivity of simulated waste solutions using standard electrochemical techniques and to improve our understanding of the corrosion mechanisms of plain carbon steel, especially pitting.

Linear polarization resistance values, which are related to the corrosion rate, were found to change with the corrosivity of simulated wastes; decreasing as the nitrate concentration was increased. These values will be used as a baseline for the analysis of the ENM. Although linear polarization resistance values can not be used to detect the onset of pitting, monitoring in the waste tanks could be used as an indicator of the increased susceptibility of the waste tanks to corrosion.

Metallographic analysis indicated that the nitrate anion appears to destabilize the oxide on the steel which leads to an increased pitting susceptibility. Pits were found to nucleate at either manganese sulfides or aluminum oxides. These inclusions were present at the surface of test samples and also became exposed after general corrosion.

J. I. Mickalonis
July, 1993

WSRC-TR-93-322

INTRODUCTION

The waste tanks that are to be used for In-Tank Precipitation (ITP) and Extended Sludge Processing (ESP) will have their present static environments changed to more dynamic conditions. These dynamic changes may cause corrosive conditions in localized areas of the tanks. Corrosion monitoring of the tanks offers the potential for identifying such conditions. An investigation was initiated to develop baseline data on the effect of changes in waste chemistry on corrosion processes of a waste tank and to support the evaluation of a new corrosion monitoring technique called electrochemical noise measurements (ENM).

Laboratory tests were conducted at Westinghouse Science and Technology Center (WSTC) to evaluate ENM for the waste tank environments at SRS. The nitrate and nitrite concentrations of simulated wastes were systematically changed to vary between inhibitive and corrosive conditions. In support of the WSTC studies, baseline testing was performed at the Savannah River Technology Center to verify the corrosivity of the WSTC simulated waste solutions using standard techniques and to improve our understanding of the corrosion mechanisms of plain carbon steel, especially pitting. Electrochemical techniques and metallographic analysis were used. This report presents the results of the SRTC tests, while the WSTC results will be reported under separate cover.

EXPERIMENTAL PROCEDURE

The test samples for this study were made from ASTM A537 plain carbon steel which is the material of construction of the most recent waste tanks. The nominal composition of this steel alloy is 0.24 %C, 0.70-1.60 %Mn, 0.040 %S, 0.035 %P, and 0.15-0.50 %Si with small amounts of Cu, Cr, and Ni. The samples were supplied by Metal Samples (Munford, AL).

The sample configurations that were used for testing were a flat, circular disk and a cylindrical rod. The circular disk is the standard test geometry for the cyclic polarization test, while the rod is an element for polarization resistance probes. Polarization resistance probes are a common corrosion monitoring technique that is used in many industries. A polarization resistance value, which is measured with a probe as well as with ENM, is related to the corrosion rate or the corrosivity of a solution.

The circular disk had approximately a diameter of 0.625 in. (1.588 cm) and a thickness of 0.125 in. (0.318 cm). The disk was punched from a rolled sheet and had an as-received surface finish of 600-grit. Each disk sample was reground prior to testing. The cylindrical rod had approximately a diameter of 0.188 in. (0.478

cm) and a length of 1.250 in. (3.175 cm). The rod was machined from a rolled plate. A hole was tapped into one end for mounting on the sample holder. The as-received surface had a 600-grit finish and was not reground prior to testing.

The corrosion tests were conducted in solutions which simulated a washed precipitate for ITP. Various nitrate and nitrite concentrations were tested to study the effect on the pitting mechanism. The base composition is shown in Table 1 and was reported in the Basic Data Report, revision 90, for ITP (1). The nitrate and the nitrite concentrations were increased by the addition of either a 5 M sodium nitrate solution or a 40 wt% sodium nitrite solution.

The corrosion process was investigated by using cyclic potentiodynamic polarization and linear polarization in conjunction with corrosion potential monitoring. The electrochemical equipment consisted of an EG&G Princeton Applied Research (PAR) Model 273 Potentiostat which was controlled by a computer data acquisition system with PAR SoftCorr Model 352 software.

The test setups were identical for the two electrochemical techniques. The test container was a Greene-type corrosion cell equipped with a gas inlet, graphite counter electrodes, thermometer, and a Ag/AgCl reference electrode. The cell was held in a heating mantle during the tests. The sample holders differed slightly for the disk and rod samples. The disk was held in a Teflon™ holder with a knife-edge gasket that exposed a surface area of 1 cm^2 to the solution. The rod was screwed onto a longer stainless steel rod which was isolated from the solution with a glass sleeve. A Teflon™ gasket was placed between the sleeve and the top of the test rod. The rod had an exposed surface area of approximately 7 cm^2.

Cyclic potentiodynamic polarization was performed on only the disk samples. Tests were conducted at 40 °C in approximately 500 mL of solution at various nitrate and nitrite concentrations. Table 2 lists these concentrations and the pH of the solutions. The vapor space in the cell was purged with nitrogen gas. The disk was placed into the solution and allowed to stabilize for 30 minutes. The tests were initiated at a potential -0.050 V versus the corrosion potential (E_{corr}). The potential was ramped at 0.6 V/hr. The vertex potential was 0.8 V (Ag/AgCl) and the final potential was 0.2 V versus E_{corr}. The samples were removed at the end of the tests, rinsed with distilled water, and blown dry. The exposed surface areas were examined for pitting. A minimum of two tests were performed for each solution composition.

Linear polarization was performed on both the rod and disk; one

test for each sample configuration. Initially, the samples were placed into a solution of the base composition. During the course of the test, the nitrate concentration was increased. The target concentrations are shown in Table 3. The final change to the test solution was the addition of sodium nitrite to sufficiently inhibit the solution. The nitrite addition was taken from draft operational safety requirements (OSR) using calculated nitrate concentrations (2). The test length for the disk was 45 days and for the rod was 70 days. The solution temperature was 40 °C. A gas flow over the top of the solution was tried initially, but was discontinued because of excessive evaporation from the cell.

For the linear polarization the potential was scanned over a range of +/- 0.010 V versus E_{corr} at a rate of 0.6 V/hr. An initial transition in the current density of approximately 0.2 uA/cm^2 was observed for both samples. The potential scan range and the direction of the scan did not affect this initial current transient. These points were removed from the database prior to calculating the polarization resistance. The remaining data displayed the expected linear relationship between potential and current density.

The tested samples were examined with and without corrosion products using a stereomicroscope and a scanning electron microscope (SEM). Energy Dispersive Spectroscopy (EDS) was used to identify elemental compositions of corrosion products. The samples were cleaned according to ASTM G 1-88, "Standard Practice for Preparing, Cleaning, and Evaluating Corrosion Test Specimens".

RESULTS

The test results from both the cyclic polarization and the linear polarization showed that the tested nitrate/nitrite concentrations were conducive for pitting of A537 when the nitrite concentrations were lower than the technical standard limit. The microstructural analysis supported the findings of the electrochemical test and highlighted the effect of nitrate/nitrite concentrations on the corrosion morphology of plain carbon steel.

Cyclic Polarization Tests

The calculated concentrations for the cyclic polarization tests are listed in Table 2. Tests A, B, and C had different nitrate concentrations with similar nitrite concentrations. For test A the nitrite concentration is that required by the technical standard for inhibition. The nitrite concentrations for tests B and C were below the technical standards requirements for the tested nitrate concentrations. Test D had a similar nitrate concentration to that of test B but a higher nitrite concentration, although below the

OSR limits. A nitrite concentration of 0.208 M is required for inhibition at a nitrate concentration of 0.181 M. The solution composition for test E was chosen to test nitrite requirements at an extreme nitrate concentration. The nitrite concentration was larger than required by the OSR (i.e., 0.658 M).

The pH of the solutions, which are given in Table 2, decreased from that of the base composition (test A) after nitrate and nitrite adjustments. Several tests were performed with the test E solution that had the pH adjusted to 9.45, which is the pH of the base composition. These tests are referred to as E^*.

Polarization scans from the cyclic polarization tests are shown in Figures 1-3. Table 4 lists E_{corr}, the passive current density (i_p), a critical potential (E_c), and a pit protection potential (E_{pp}) that were measured from the scans. The polarization scan for test A as shown in Figure 1 indicated that the steel was passive. Passivity initiated at a E_c of 0.17 V with a i_p of 0.3 uA/cm^2. A small hysteresis loop was present in the transpassive region; E_{pp} was approximately 0.650 V.

Several changes occurred in the polarization scans when the nitrate concentration was increased for tests B and C. Figure 2 shows a representative polarization curve for these tests. The E_{corr} shifted to more active values and the i_p increased with the nitrate concentration as shown by the values in Table 4. E_c appeared more like a pitting potential since at more noble potentials the current density increased with the potential (i.e., i_p was not constant). The nitrate anion appears to destabilize the oxide during formation at E_c, so the pitting resistance of the steel is decreased.

Test D had a similar nitrate concentration to test B and a higher nitrite concentration which was still below the technical standard requirement. E_{corr} for test D shifted to more active potentials than those for tests A-C. The i_p was similar to those for test B. A E_{pp}, however, was observed for one of the runs as shown by the polarization scan in Figure 3. The occurrence of E_{pp}, which was not observed in test B, was attributed to an increased inhibition of the higher nitrite concentration. The test results for test D indicated that the conditions were borderline for inhibition.

For test E the nitrite concentration was greater than that required for inhibition by the technical standard, although at high nitrate concentrations. The polarization curves from these tests were similar to that shown in Figure 3. The low and constant value of the i_p indicated a sufficient nitrite concentration was present for inhibition. The higher nitrate concentration, however, eventually caused pitting as evidenced by a hysteresis loop.

Similar results to test A were initially expected since both nitrite concentrations were above the technical standard requirement for inhibition. The results, however, showed that the test E solution was more corrosive. A possible contributing factor was the solution pH.

The effect of pH on the polarization results was investigated with the solution composition of test E. The test results are given in Table 4 and are labelled as E^* and E^{**}. The E^* solution was adjusted to a pH of approximately 9.45 and that for E^{**} was the same as for test E. E^{**} tests were performed since the E^* tests were performed using a different batch of the base solution. A comparison of E^* and E^{**} results indicated that a lower pH caused a shift of E_{corr} to more electronegative values and of i_p to larger average values. A decrease in pH, therefore, lowered the corrosion resistance of the steel and was probably a contributing factor to the differences observed between tests A and E. The differences in the results from tests E and E^{**} were attributed to compositional variations of the solutions.

Linear Polarization

The linear polarization test results were different for the disk and the rod although both samples corroded in the higher nitrate solutions. The polarization resistance (R_p) and E_{corr} are shown graphically in Figures 4 and 5 for the disk and rod, respectively. The times of the nitrate additions are indicated along the bottom of the graphs with arrows and differ slightly for the disk and rod.

For the disk, an increased corrosivity at higher nitrate concentrations was indicated by a decrease in R_p and a shift in E_{corr} to more active values. During the initial ten day period the sample was allowed to stabilize. E_{corr} was stable at approximately 0.09 V; however, R_p was more variable. Discounting the initial transition, an average value of 50 kohms/cm was obtained. Subsequent changes in E_{corr} and R_p did not correlate well with the additions of nitrate to the solution. This result may have been from the short test period with frequent disturbances of the solution (i.e., insufficient time for the sample to stabilize). By the end of the test, however, E_{corr} had shifted to potentials in the range of -0.1 to -0.2 V and R_p had an average value of 25 kohm/cm.

The test for the rod was changed to allow more time for R_p and E_{corr} to stabilize. The first addition was made 30 days after the rod was placed into the solution. E_{corr} stabilized at approximately 0.04 V; while R_p increased to approximately 200 kohm/cm. The nitrate concentration was increased to 0.184 M at the first addition, which was unlike the smaller addition with the disk. E_{corr} was not affected by this change, but R_p dropped to approximately 125 kohm/cm. R_p

decreased to approximately 90 kohm/cm at a nitrate level of 0.28 M. Again, E_{corr} was not affected. The last nitrate addition to 0.704 M, however, appeared to cause a perturbation in E_{corr} as shown in Figure 4. Afterwards, E_{corr} returned to the same value. R_p decreased to 40-50 kohm/cm. The last addition to the solution increased the nitrite concentration to 1.084 M, which was calculated from the inhibition requirements of the technical standard. The E_{corr} and R_p did not change.

The general trends of R_p for the disk and rod were similar, decreasing with increasing nitrate concentration. The trends in E_{corr}, however, were different, although the initial potentials were similar. The disk potential became more electronegative, while for the rod E_{corr} remained fairly constant. The difference may be due to a surface area or geometric effect. A small amount of pitting will cause a smaller change in the potential of a larger sample. From qualitative observations of the surface as discussed below, the disk did appear to have a greater amount of corrosion. Another possible factor is the larger interfacial area between the disk sample and the holder than that for the rod. This area is susceptible to crevice corrosion which will cause E_{corr} to be more active.

Microstructural Analysis

A microstructural analysis was performed on the samples that were used in this study to identify the corrosion morphology and to investigate correlations between the morphology and the microstructure of the sample. In general, pitting was the dominant corrosion process although crevice and general corrosion also occurred. Various initiation sites for pitting were found indicating an effect of both the surface condition and the microstructure.

Microstructural Characterization Of Samples

The electrochemical disks and rod electrodes had differing initial surface conditions and microstructures. These differences occurred from the material processing and specimen preparation procedures. According to the supplier, the disks were machined from 1/8-in. plate and the rods were machined from 1/4-in. plate. The microstructure of the exposed surface depended on the orientation of the sample relative to the rolling direction of the plate.

For the disks, two different microstructures were observed as shown in the micrographs of Figure 6. Figure 6A shows a laminar microstructure of ferrite and pearlite found in the two test samples from the cyclic polarization tests that were examined. The disk that was used for the linear polarization tests had the

microstructure shown in Figure 6B. Both microstructures contained inclusions as shown in the SEM photomicrograph of Figure 7 for the linear polarization sample. The corresponding energy dispersive spectra are given in Figure 8.

The rod electrode had a laminar microstructure in the transverse and cross sectional directions as shown by the micrographs in Figure 9. Aluminum oxide and manganese sulfide inclusions were also found. The microstructure of the exposed surface of the rod would be more complex since it would vary around the circumference of the sample.

Both the rod and the disks were prepared to a 600-grit surface finish, but the rod had a coarser appearance. Gashes were present on the surface of the rod, but were not on that of the disk. The rod was prepared by the manufacturer, while the disks were prepared in the laboratory immediately prior to testing.

Corrosion Morphology Of Cyclic Polarization Disks

Several forms of corrosion occurred on the disks from the cyclic polarization tests. The corrosion processes were pitting, crevice corrosion under the sample holder gasket, and general corrosion. Descriptions of the examined test samples are given below. The test samples were examined, at a minimum, with a stereomicroscope. The SEM investigation with EDS was performed on a more limited basis.

The samples in the base solution (test A), which was characterized as inhibitive, were fairly free of corrosion. A slight discoloration was observed, but may have resulted from the rinsing procedure after the test. These samples were examined with the stereomicroscope only.

The samples from test B had a "swiss cheese" appearance with pitting. The "swiss cheese" areas showed general attack with a number of small pits (5-10 microns). These pits probably initiated either at exposed subsurface inclusions or in deep troughs which resulted from the general attack. The photomicrograph in Figure 10 shows an area of general attack.

Pits had either rounded or elliptical shapes. Most of the examined pits were associated with some type of inclusion, either aluminum oxide or manganese sulfide. The aluminum oxide inclusions also contained smaller amounts of magnesium and calcium. These particles may have come from the retention of slag. Many of the pits were in linear arrays as shown in the photomicrograph of Figure 11. The corrosion products on the surface were identified as iron oxides.

Crevice attack under the gasket was found on the B samples. The

attack at grain boundaries in these regions was significant and may be associated with impurities. Pitting was also observed. The variation in the polarization scans for the test B solution may have resulted from a varying degree of crevice corrosion.

Pitting was more significant with the test C solution which had a higher nitrate concentration than the previous tests. Pits were approximately 5-10 microns, although they appeared slightly deeper than those on test B samples. The pits had domes of corrosion products similar to those shown in Figure 12 for test E samples. The degradation of test C samples did not appear as severe as that observed on test B samples. The more extensive general attack that occurred in test B may have caused this anomaly. Some crevice corrosion at the gaskets was also observed on test C samples.

Test D samples had different corrosion morphologies as indicated by their differing polarization results. The sample which had a curve indicating only active corrosion did have pits on the exposed surface although severe crevice corrosion also occurred. The other sample had pits as described previously for test C samples. The D test samples were the first to be found with mercury particles on the surface, which are shown in Figure 13.

Test E samples had pit morphologies similar to those of test D samples including the presence of mercury particles. Pitting of the test E samples did not appear significantly different from those of test D. Crevice corrosion at the gasket was also found on the test E samples.

Corrosion Morphology of Linear Polarization Samples

The morphology and extent of corrosion differed for the disk and the rod. A macroscopic photograph of the test samples is shown in Figure 14. The corrosion of the disk was greater than that of the rod even though the test length for the disk was shorter. The differences in the corrosion may have been due to several factors. These factors include variation in solution chemistry, sample geometry, surface preparation, or sample microstructure.
The corrosion on the disk was concentrated at the perimeter of the exposed area near the gasket region. The rod had a tarnished appearance with minimal corrosion products. Regions near the top of the rod were more severely attacked than those near the bottom although this difference is not apparent in the figure.

The corrosion products on the disk had a crusty appearance with particulate matter of variable size as shown in Figure 15. EDS analysis revealed that the crusty regions were composed of iron and aluminum oxides. Sodium and sulfur species were also present. The larger particulates were primarily aluminum oxides with smaller

amounts of potassium, calcium, magnesium, and silicon. The small white particles in the micrograph are composed of mercury and silver. The origin of the silver is unknown.

After the corrosion products were removed, pitting and general corrosion were found. Most of the pitting was associated with aluminum oxide and manganese sulfide inclusions as observed on the cyclic polarization samples. In several regions the grains appeared to be preferentially attacked as shown in Figure 16. If this attack revealed an inclusion, pitting appeared to be initiated. Some particles containing mercury and silver were still present even after cleaning.

The corrosion products on the rod were primarily iron oxides although aluminum and silicon were also detected. Cleaning the rod did not greatly change its appearance since only a minimal amount of corrosion product was present. Pitting was the prevalent corrosion mechanism. The pits did not have caps of corrosion products as observed on some of the cyclic polarization samples. The pits were found, however, to be in linear arrays and have either round or slightly elongated shapes. Some pitting initiated at surface gashes as shown in Figure 17.

CONCLUSIONS

Corrosion monitoring of the waste tanks is necessary to minimize the corrosion when the conditions are near the OSR limits. This study has shown that the severity of pitting and general corrosion increased with the nitrate concentration. The dynamic conditions that will occur during waste processing, such as varying nitrate and nitrite concentrations, make corrosion monitoring more critical.

This study has provided a better understanding of the pitting mechanism of plain carbon steel exposed to waste tank environments. The results indicated that the nitrate anion appears to destabilize the oxide on the steel which leads to an increased pitting susceptibility. Metallographic analysis showed that pits nucleate at either manganese sulfides or aluminum oxides. These inclusions are present at the surface or may become exposed after general corrosion occurs. Pits may also be initiated at surface flaws.

A common technique for corrosion monitoring is a polarization resistance probe which is similar to that used for ENM. These probes use rod-shaped electrodes as were used in this study. The test results showed that R_p values are correlated with changes in the corrosivity of simulated wastes; decreasing as the nitrate concentration was increased. These values will be used as a baseline for the analysis of the ENM. Although R_p values can not be

used to detect the onset of pitting, monitoring of R_p in the waste tanks could be used as an indicator of the increased susceptibility of the waste tanks to corrosion.

Since polarization resistance probes can not be used to detect localized corrosion, the development of other techniques such as ENM is necessary for waste tank application. ENM is currently being evaluated with WSTC for SRS waste tanks. The combination of polarization resistance and ENM will potentially form the basis of a comprehensive strategy to monitor the corrosion susceptibility of waste tanks under dynamic conditions.

REFERENCES

1. Basic Data Report Defense Waste Processing Facility Sludge Plant, DPST-80-1033, volume 2, revision 90, October 30, 1984.

2. Westinghouse Savannah River Company, Operational Safety Requirements In-Tank Precipitation Process Savannah River Site (U), WSRC-RP-93-1124, draft 4/92.

Table 1. Composition Of Simulated ITP Washed Precipitate Solution (BDR-90)

Constituents	Concentration (M)
Aluminum Nitrate	2.05E-2
Iron Nitrate	5.50E-3
Sodium Hydroxide	9.37E-2
Sodium Nitrate	5.18E-3
Sodium Nitrite	2.57E-2
Sodium Oxalate	8.66E-3
Sodium Sulfate	5.94E-3
Sodium Carbonate	5.80E-2
Sodium Bicarbonate	1.20E-2
Sodium Hypophosph.	3.90E-4
Calcium Carbonate	6.60E-4
Sodium Chloride	1.03E-3
Sodium Fluoride	7.30E-4
Sodium Chromate	1.40E-4
Chromium Chloride	6.00E-5
Sodium Molybdate	1.85E-5
Sodium Metasilic.	1.60E-4
Uranyl Nitrate	3.30E-4
Cobalt Nitrate	1.50E-6
Copper Nitrate	2.00E-5
Manganese Dioxide	1.14E-3
Nickel Nitrate	5.20E-4
Mercury Nitrate	1.10E-4
Zinc Nitrate	4.00E-5
Lead Nitrate	2.00E-5
Phenol	4.30E-6

Table 2. Nitrate and Nitrite Concentrations[1] For Cyclic Polarization Tests

Test	Nitrate[2] Concentration (M)	Nitrite[3] Concentration (M)	pH
A	0.022	0.030	9.46
B	0.184	0.029	9.34
C	0.310	0.028	9.27
D	0.181	0.161	9.25
E	0.549	0.946	9.00
E*	0.55	0.95	9.45
E**	0.55	0.95	9.00

1. Concentrations were calculated.

2. Nitrate concentration increased by addition of 5 M sodium nitrate solution to base solution composition.

3. Nitrite concentration increased by addition of 40 wt% sodium nitrite solution to base solution composition.

Table 3. Target Concentrations[1] Of Nitrate and Nitrite For Polarization Resistance Tests

Addition	Nitrate[2] Concentration (M)	Nitrite[3] Concentration (M)
0	0.022	0.030
1	0.037	0.03
2	0.0797	0.0297
3	0.184	0.029
4	0.298	0.028
5	0.704	0.026
6	0.64	1.086

1. Concentrations were calculated based on initial composition and quantity of additional solution.

2. Nitrate concentration increased by addition of 5 M sodium nitrate solution to base solution composition.

3. Nitrite concentration increased by addition of 40 wt% sodium nitrite solution to base solution composition.

Table 4. Electrochemical Pitting Parameters From Cyclic Polarization Tests

Test	E_{corr} (V Ag/AgCl)	i_p (uA/cm^2)	E_c (V Ag/AgCl)	E_{pp} (V Ag/AgCl)
A	0.050	0.3	0.17	--
	0.062	0.3	0.17	--
B	-0.129	3.2	0.17	--
	-0.132	3.2	0.17	--
C	-0.161	>10	0.17	--
	-0.124	>10	0.17	--
D	-0.175	3.2	0.17	--
	-0.243	1.0	0.17	0.575
E	-0.267	1.0	0.17	0.550
	-0.291	1.0	0.17	0.525
E*	0.090	3.2	0.17	--
	0.137	1.0	0.19	--
E**	-0.031	3.2	0.17	--
	0.007	3.2	0.16	--

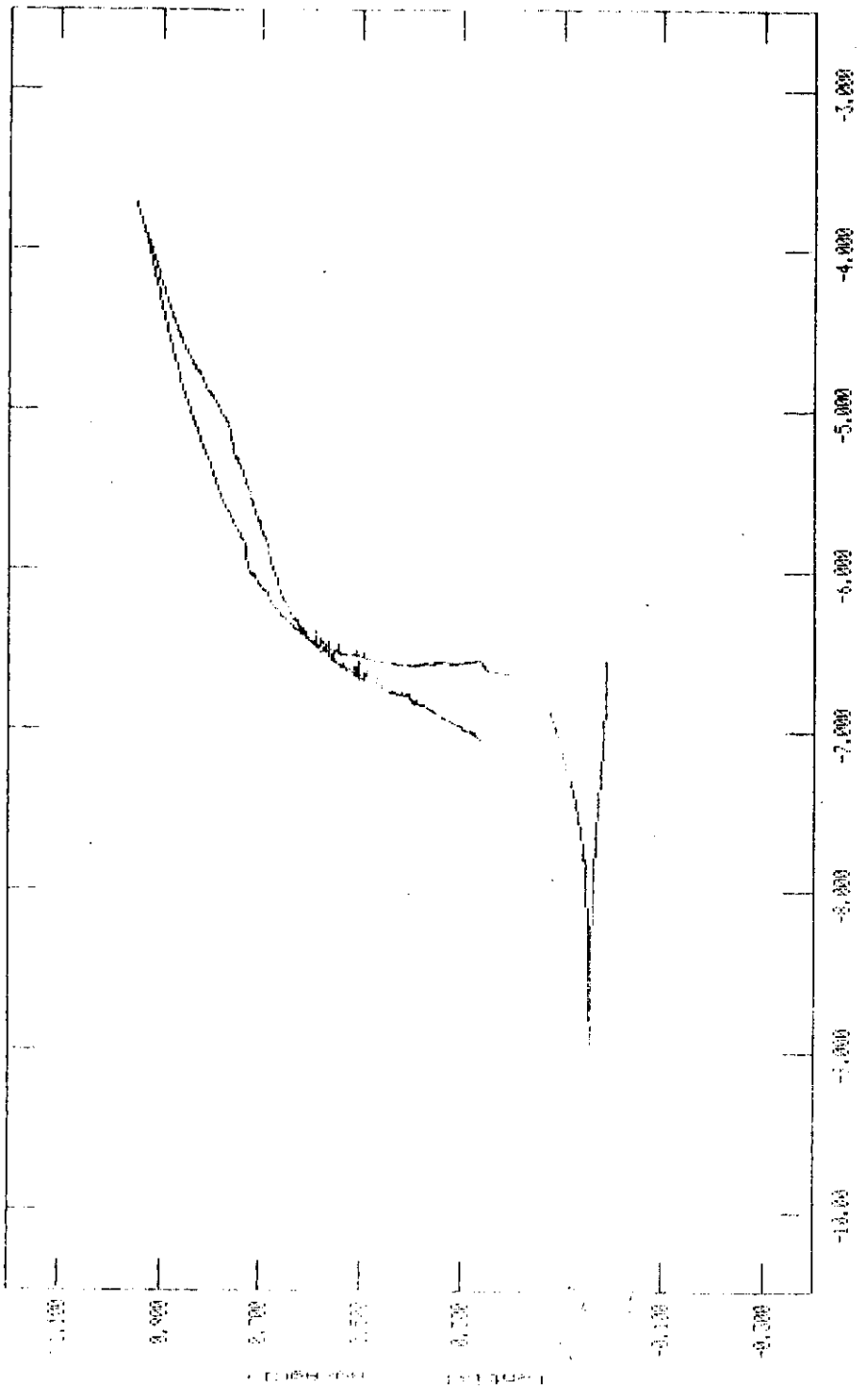

Figure 1. Polarization scan for A537 plain carbon steel in a simulated ITP washed precipitate solution with 0.022 M sodium nitrate and 0.031 M sodium nitrite (Test A)

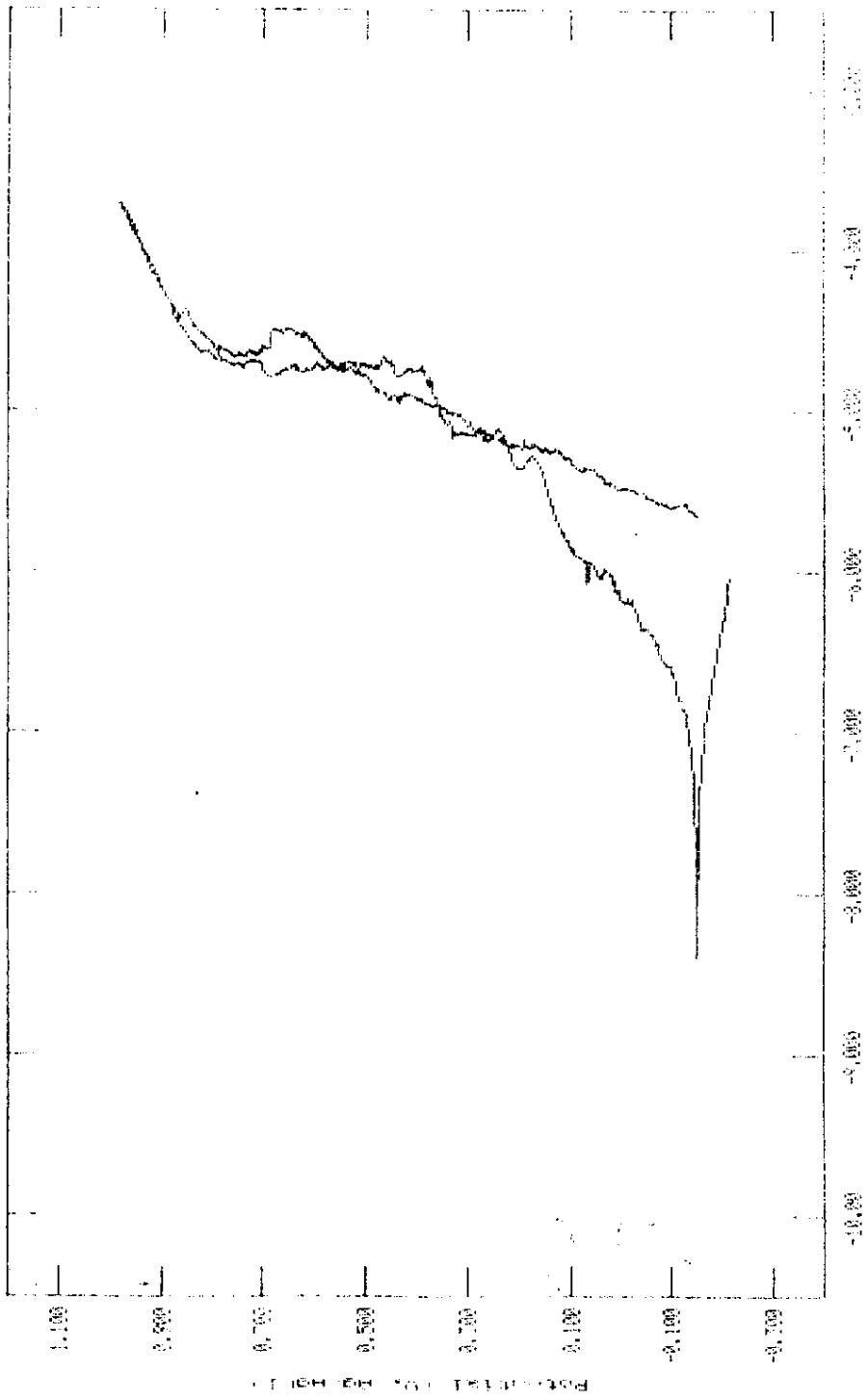

Figure 2. Polarization scan for A537 plain carbon steel in a simulated ITP washed precipitate solution with 0.310 M sodium nitrate and 0.028 M sodium nitrite (Test C)

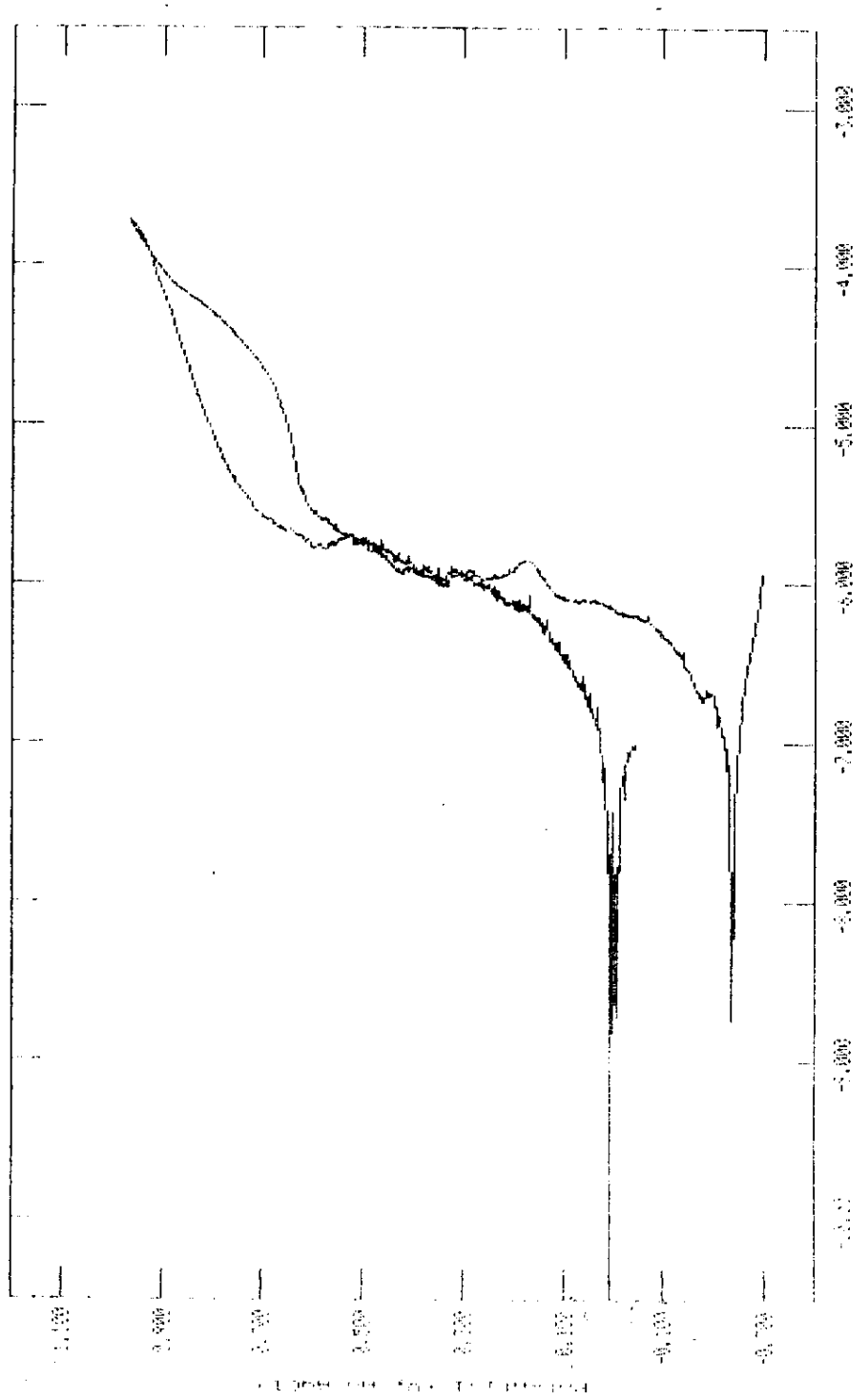

Figure 3. Polarization scan for A537 plain carbon steel in a simulated ITP washed precipitate solution with 0.181 M sodium nitrate and 0.161 M sodium nitrite (Test D)

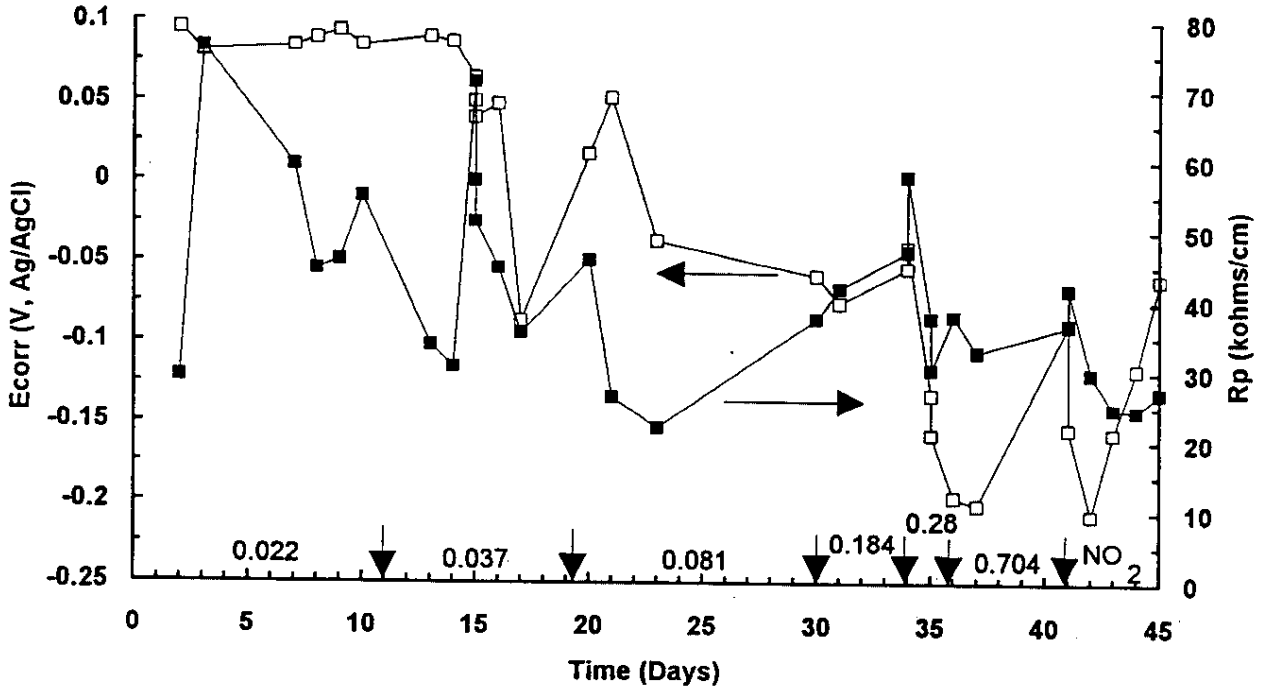

Figure 4. E_{corr} and R_p measurements with a disk sample of A537 plain carbon steel

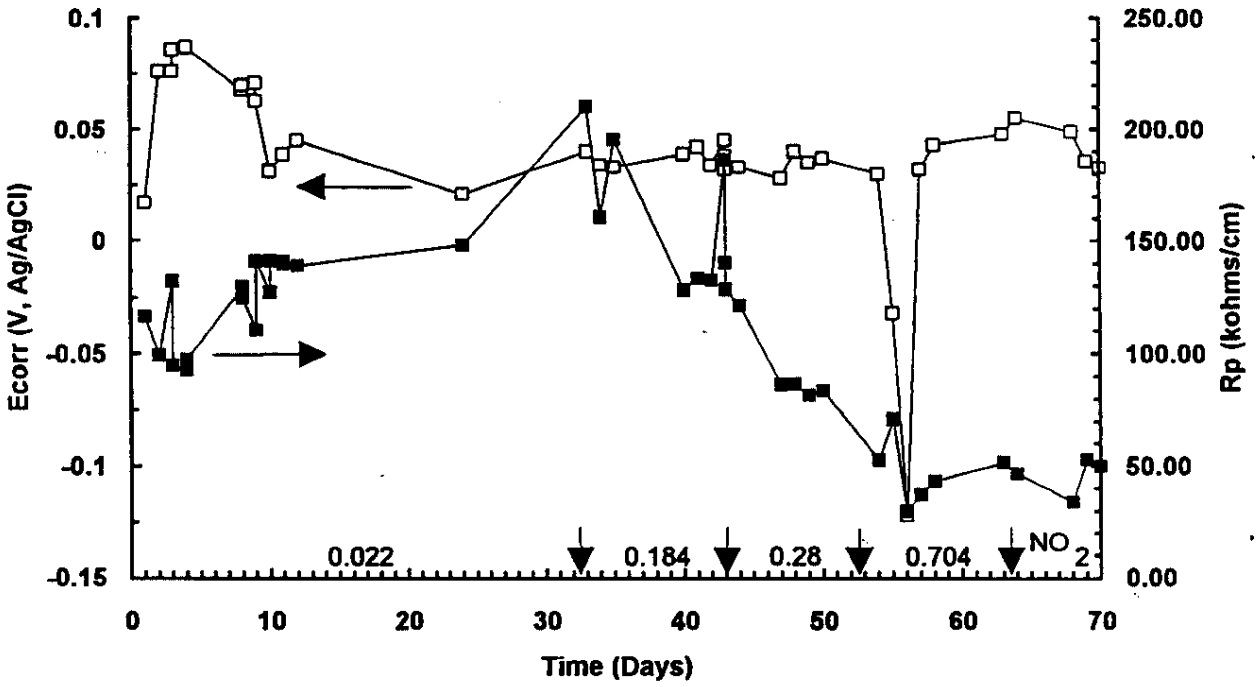

Figure 5. E_{corr} and R_p measurements with a rod sample of A537 plain carbon steel

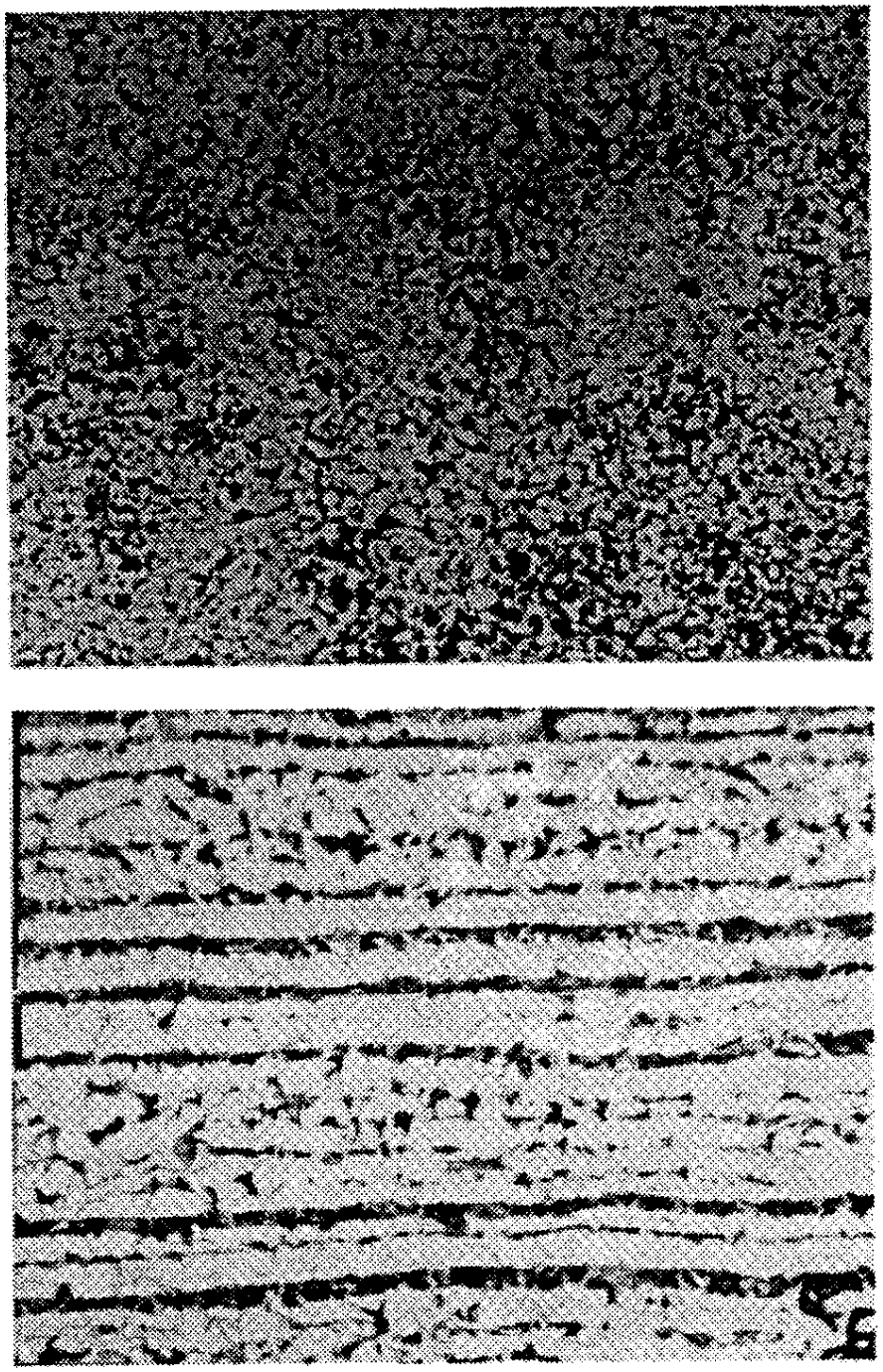

Figure 6. Micrographs displaying the various microstructures of A537 plain carbon steel disks.

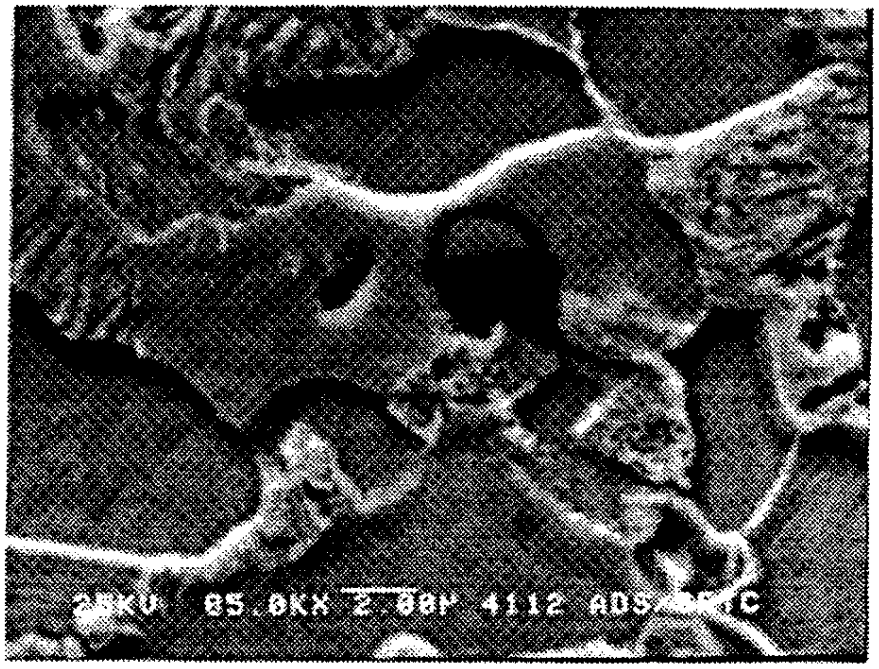

Figure 7. SEM photomicrograph inclusions in A537 plain carbon steel rod samples.

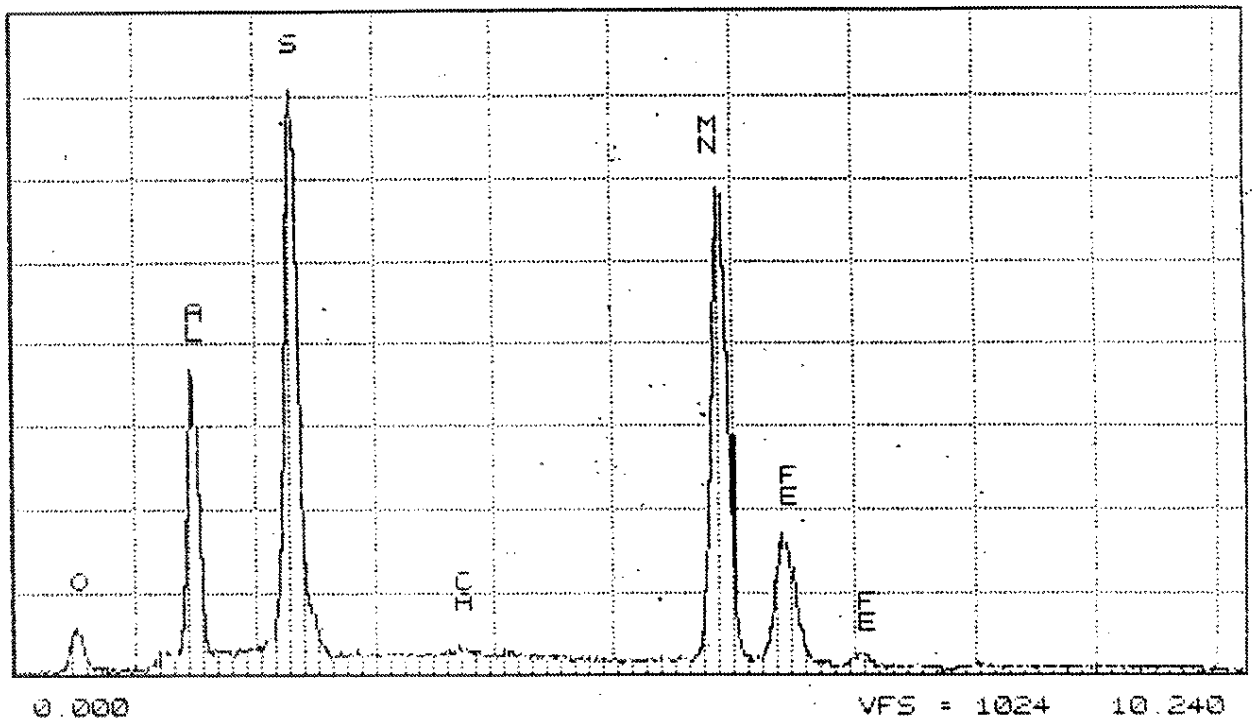

Figure 8. EDS spectra of inclusion shown in Figure 7.

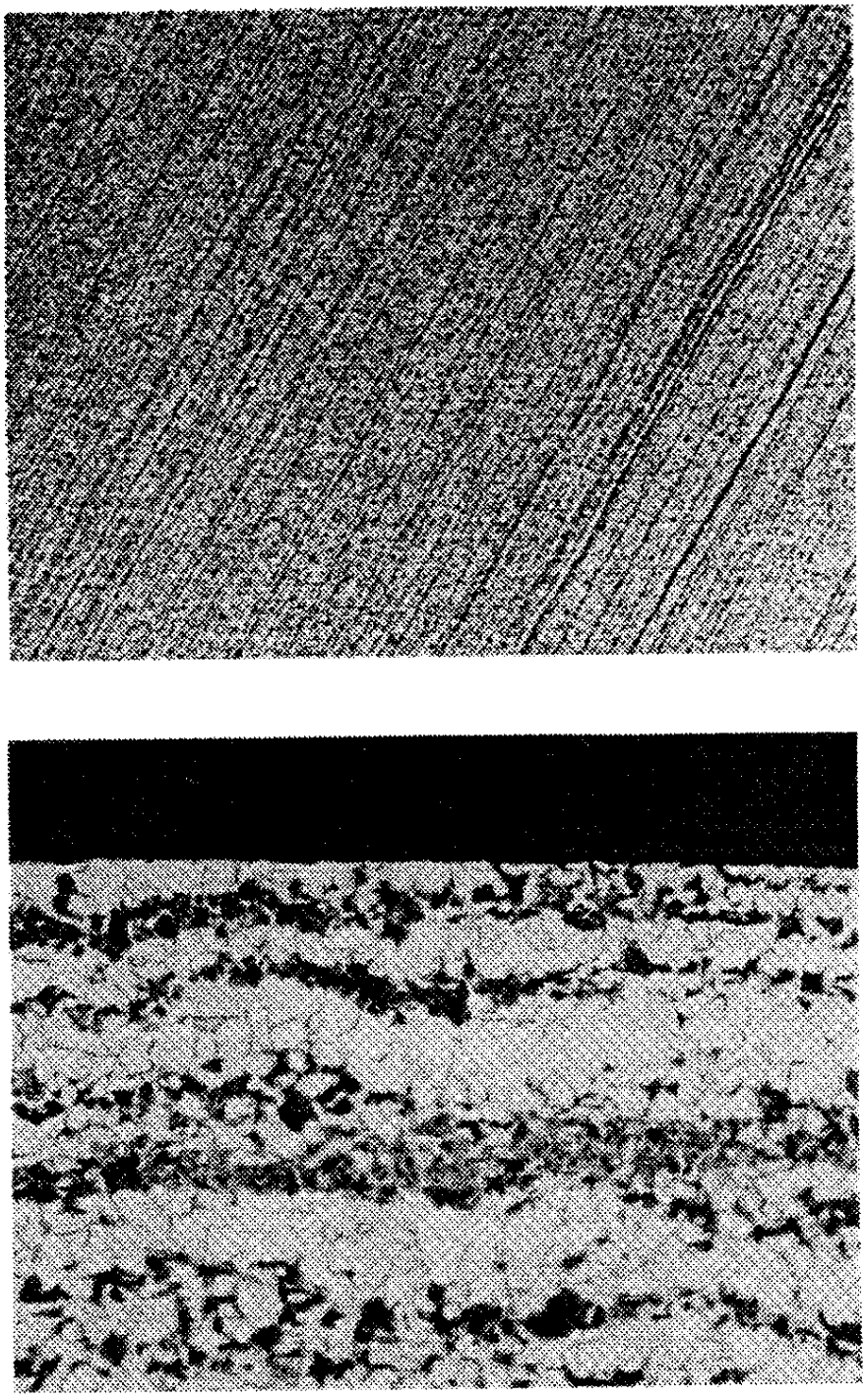

Figure 9. Photomicrograph displaying transverse (A) and cross-sectional (B) views of the microstructure of a A537 plain carbon steel rod.

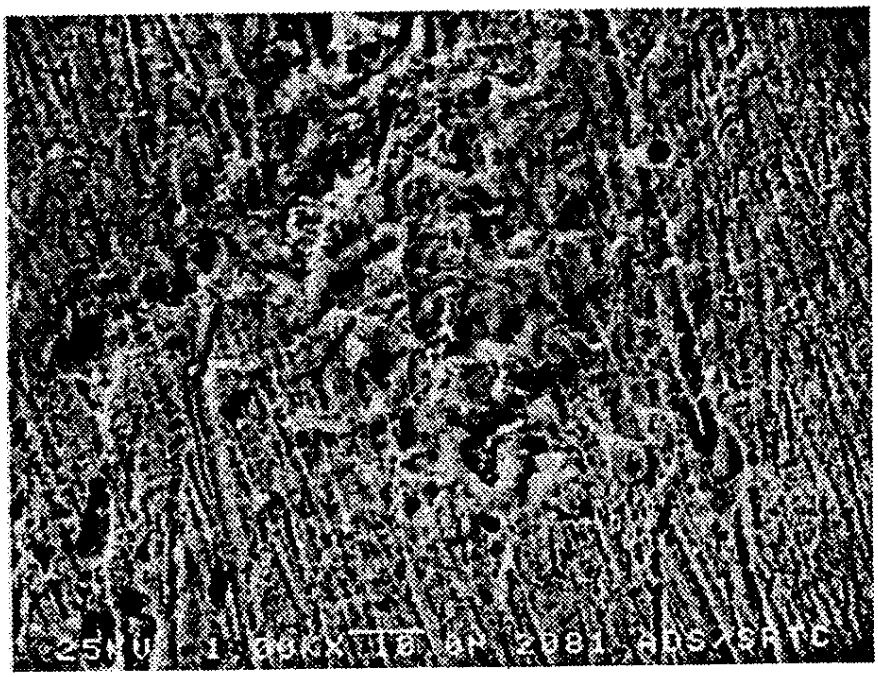

Figure 10. SEM photomicrograph of an area of general corrosion on the disk sample from test B.

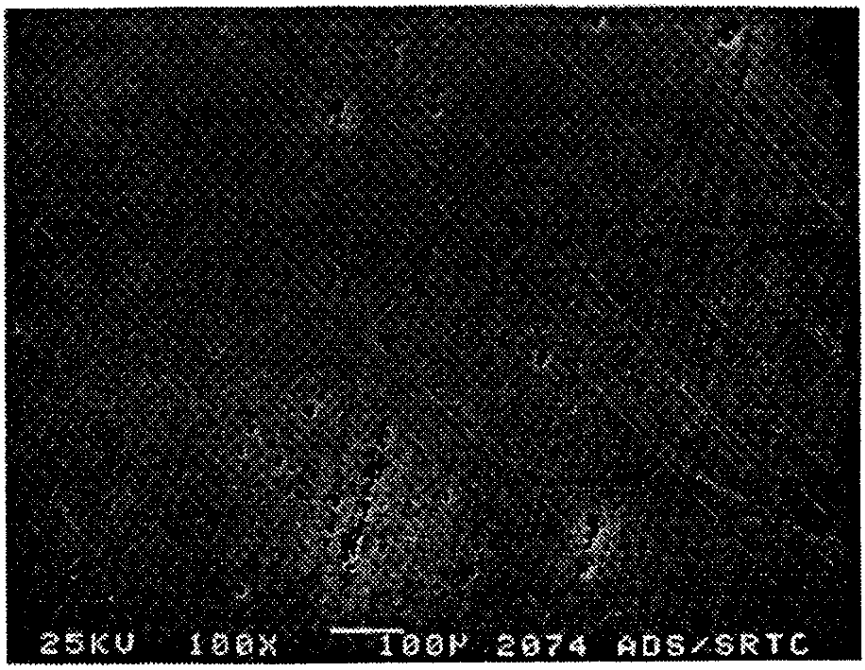

Figure 11. SEM photomicrograph of a linear array of pits on a disk sample from test B.

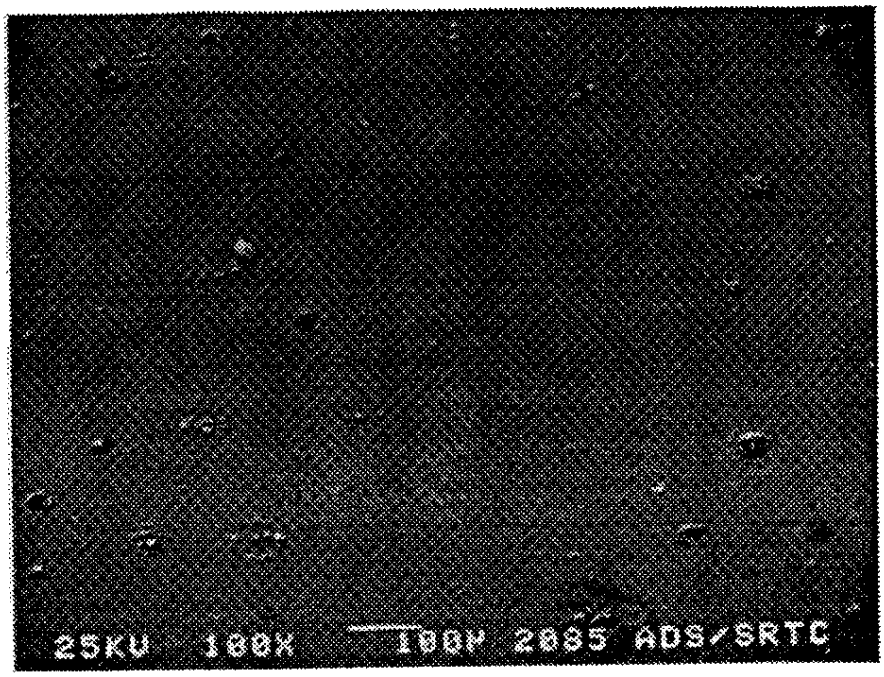

Figure 12. SEM photomicrograph of pits covered with corrosion products on a disk sample from test E.

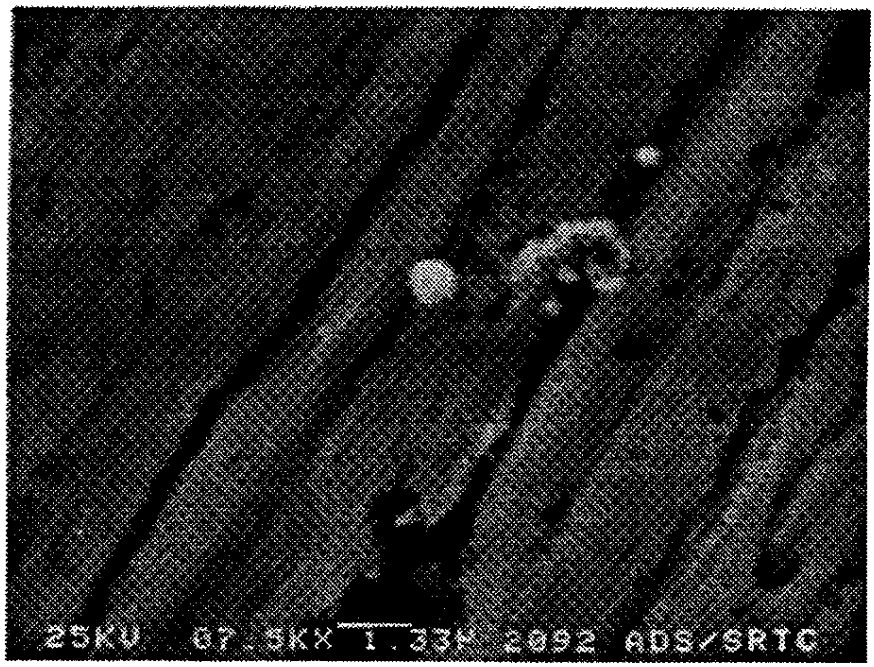

Figure 13. SEM photomicrograph of mercury particles on a sample from test D.

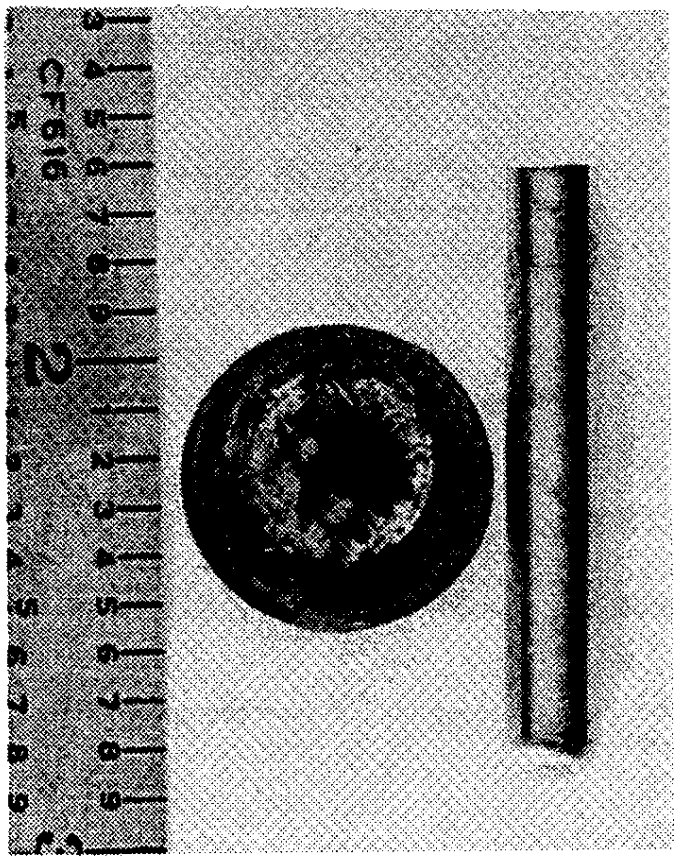

Figure 14. Photograph displaying the rod and disk samples used in the linear polarization test.

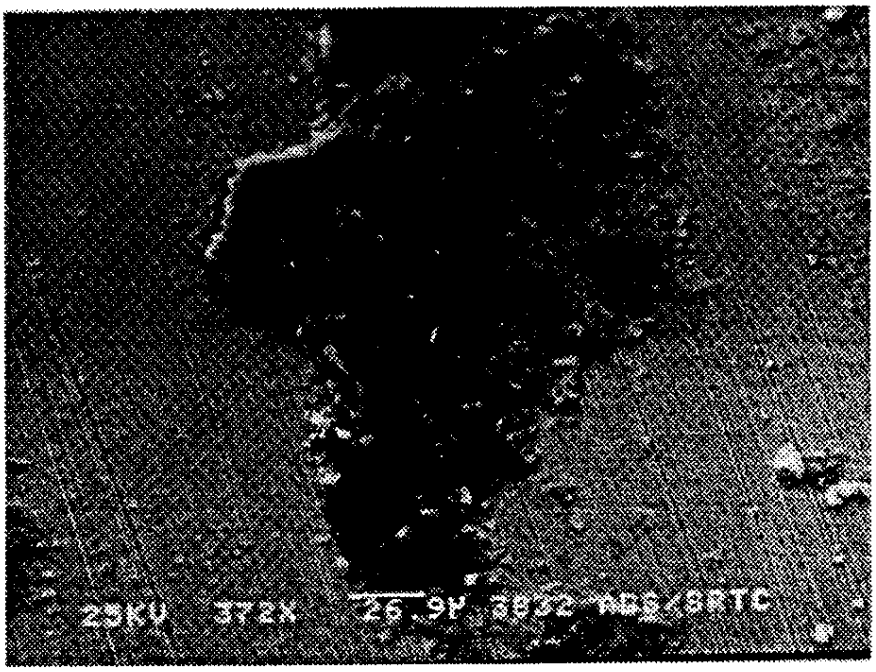

Figure 15. SEM photomicrograph displaying the corrosion products that formed on the disk sample from the linear polarization test.

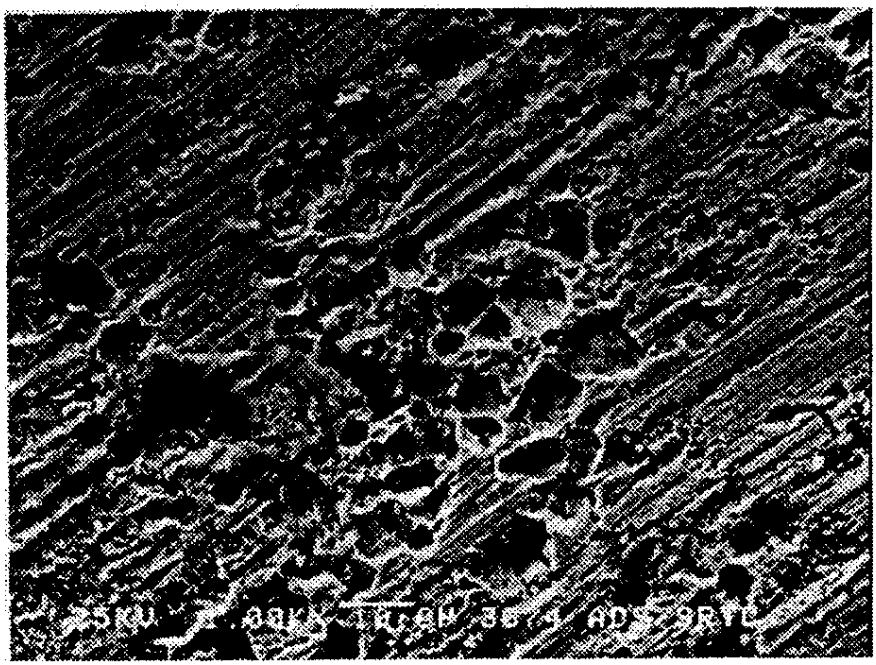

Figure 16. SEM photomicrograph displaying an area ofpreferential grain attack on the rod sample from the linear polarization.

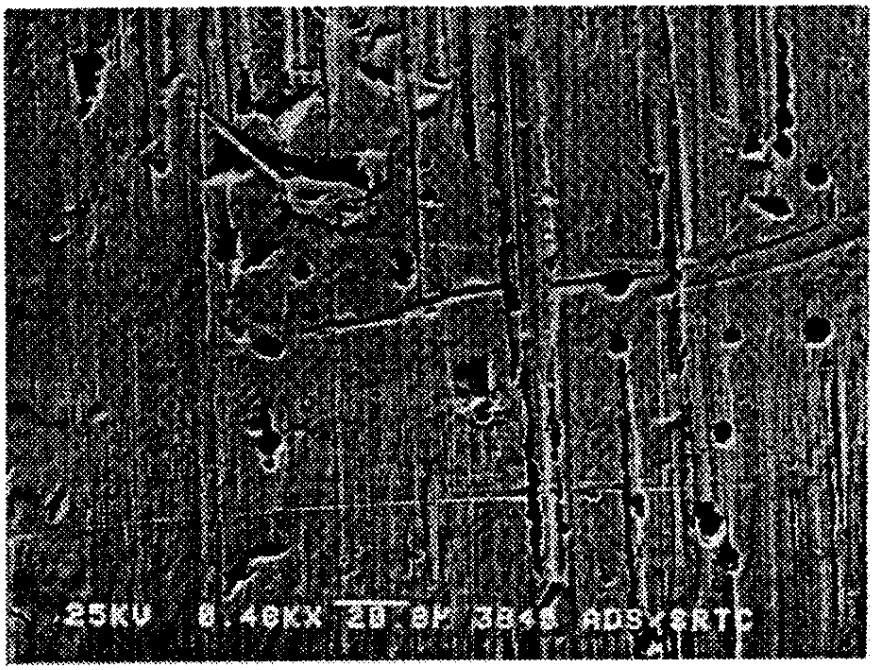

Figure 17. SEM photomicrograph displaying a pit at a surface gash on the rod sample from the linear polarization test.

DISTRIBUTION:

J. E. Marra, 703-H
B. L. Lewis, 703-H
J. R. Chandler, 703-H
T. C. Hsu, 703-H
D. T. Hobbs, 773-A
T. L. Capeletti, 773-41A
N. C. Iyer, 773-A
C. F. Jenkins, 730-A
K. J. Imrich, 773-A
B. J. Wiersma, 773-A
P. E. Zapp,773-A
SRTC Records, 773-[redacted]A (4)
MTS Files, 773-A, D-1155